N89-24550

Turbulence production near walls: the role of flow structures with spanwise asymmetry

By P. Henrik Alfredsson[1], Arne V. Johansson[1] and John Kim[2]

Space-time evolution of near-wall flow structures is described by conditional sampling methods, in which conditional averages are formed at various stages of development of shear-layer structures. The development of spanwise asymmetry of the structures was found to be important in the creation of the structures and for the process of turbulence production.

1. Introduction

Over the past two decades, the results from the pioneering flow visualization studies of the near-wall structure (e.g. Kline et al., 1967; Kim, Kline & Reynolds, 1971) and the resulting conceptual model of the various stages of the 'bursting' process has has remained as a cornerstone in our views of turbulence production in boundary layers. A central part of the model is the localized lift-up of low-speed fluid from the viscous sublayer into the buffer region, which creates strong, more or less symmetric (with respect to the spanwise center of the low-speed region) internal shear layers coupled to a velocity profile with inflectional character. The flow-visualization results indicated that a major portion of the turbulence production occurs during violent break-up of the flow structure into small scales, which was believed to originate from an inflectional instability giving rise to a growing oscillation of the lifted low-speed region. The conceptual model does not, however, account for regeneration of the low-speed regions in the viscous sublayer.

From flow-visualization studies and subsequent probe measurements it was concluded that a great portion of the turbulence production occurs during highly intermittent events. A mean time between consecutive events could be determined, and was found to be much larger than their duration. Hence, turbulence production was concluded to be strongly intermittent both in time and space. One should note, however, the inherent difficulty in flow visualization, using hydrogen bubble, dye or other techniques, to follow a specific structure or process for long times, because all path lines diverge rapidly in a turbulent flow. Also, structures need not be simply advected, but may propagate in somewhat of a wave-like manner through the action of pressure. The conditionally-averaged data indicate that there is no apparent sign of the break-up stage with associated small-scale motions. This is, however,

1 Royal Institute of Technology

2 NASA Ames Research Center

somewhat inherent in the conditional averaging methods, because motions of small or large scale that are weakly correlated or uncorrelated with the primary feature, on which the detection is focused, will be averaged out in the ensemble-averaging process. Large contributions to the Reynolds stress have mainly been found directly associated with the lift-up of low speed fluid, i.e. on the downstream side of the shear layer (Johansson et al. 1988).

Probe methods have been used to map some of the spatial features of the structures. For instance, Johansson et al. (1987a) analyzed two-probe measurements from the Göttingen oil-channel with the VITA-technique, which focused on the shear-layer structure of a certain size and strength. Information from only one xy-plane was available from the experiment. Obtaining a complete space-time mapping in three dimensions experimentally would be an extremely difficult task, but can in principle easily be done with the use of numerical data bases obtained from simulations. Johansson et al. (1988) used the NASA Ames computer-generated numerical data bases of turbulent channel flow, which has a spatial resolution of 17.7 and 5.9 viscous units in the streamwise (x) and spanwise (z) directions, respectively, to do space-time mapping of the shear-layer structures detected by the spatial counterpart of VITA. The Reynolds number based on friction velocity (u_τ), channel half-height (b) and kinematic viscosity (ν) is 180 close to that in the Göttingen oil-channel data, and excellent agreement with the measured data was obtained.

In the present study the NASA Ames numerical data bases are further utilized for space-time mapping of the near-wall structures. For this purpose 47 flow fields separated by three viscous time units were used. The present results shed new light on the near-wall structure of turbulent flows, and show that several of the long-lived views based on early flow visualization and probe measurements may need to be modified. It is also shown that the turbulence production is less intermittent in time than previously believed. Asymmetry of the structures is also found to be an important aspect of the whole process.

2. Results

2.1 Space-time evolution of the structures

Shear-layer structures were detected with the VISA method as follows. First, 'islands' of high local variance in the xz- plane at $y^+ = 15$ were identified. Then, the maximum within each island was used as the detection point. In this way the events were aligned in the streamwise and spanwise directions before ensemble averaging. The evolution of the structures was studied by tracking the islands of high local variance between consecutive flow fields. The structures were found to be quite persistent and could often be followed over streamwise distances of the order of 1000 viscous units (see Johansson et al. 1988).

All structures detected† at a chosen time were tracked forward as well as backward in time to locate the space-time position of maximum shear-layer strength

---

† with a VISA-threshold of $1.0u^2_{rms}$ and an averaging length of 200 viscous units.

(here taken as the maximum local variance) for each event. These space-time positions were then used to construct a conditionally averaged structure at 'maximum strength'. Similarly, conditional averages could be constructed at other stages of development. The events were tracked back to an 'early' stage, which we took to be the instant when the variance just exceeded $0.7u_{rms}^2$, and similarly for a late stage. The streamwise velocity patterns in the xy-midplane at these three stages of development clearly show the strong variation in strength of the velocity pattern on the upstream, 'sweep-side' of the shear-layer (figure 1). At late stages this part becomes quite weak, whereas the downstream, 'ejection-side' retains an almost constant strength over the observed evolution. This is true, not only for the streamwise velocity disturbance, but also for the associated uv-pattern. Indeed, the uv-contribution on the upstream (sweep-type) side of the shear-layer was found to be almost negligible in comparison with that on the ejection side.

The slope of the shear-layer at the detection point can be related to the 'age' of the structure. The angle of inclination decreased from a value of 17° at the early stage to 15° and 12° at maximum strength and the late stage, respectively. This is a manifestation of the stretching and tilting of the structure by the mean shear. The corresponding angles from the v-patterns show a similar evolution (although more accentuated), in which the 'early'-stage angle is as large as about 45°.

No signs of small scale oscillatory motions (or violent break-up) were found in conjunction with the late stages of development of the main structure; we confirmed this conclusion by following several individual events. Instead, the dominating part of the associated uv-contribution resulted from the persistent uv-peak on the downstream side of the shear-layer in the Lagrangian frame of reference, which is in contrast to the above-mentioned conceptual picture of the 'bursting' process.

The pressure patterns associated with the structure are shown in figure 2 for the three stages of development described above. It can be seen that an intense localized high-pressure region develops around and beneath the centre of the shear-layer. At maximum strength the maximum amplitude (deviation from the mean pressure) is about $2.9\tau_w$, or about $2p_{rms}$. These strong localized high-pressure regions could be of significant importance for boundary-layer noise generation. One should note that the actual amplitude is affected by 'phase jitter' in the conditional averaging process, i.e. the variation in the pressure-peak position relative to the detection position, determined from the maximum in local variance.

2.2 Removal of phase jitter

There are several types of difficulties in obtaining quantitatively accurate conditional averages of the various flow variables associated with the structure. The problem of phase jitter in the conditional averaging of quantities other than that on which the actual detection algorithm is applied has, for instance, been addressed by Blackwelder (1977). Johansson et al. (1987b) used a cross-correlation technique between the individual events and the ensemble average, which was shown to be quite effective in removing the phase jitter. It resulted in, among other things, a substantially increased amplitude of the wall-pressure peak associated with the structure.
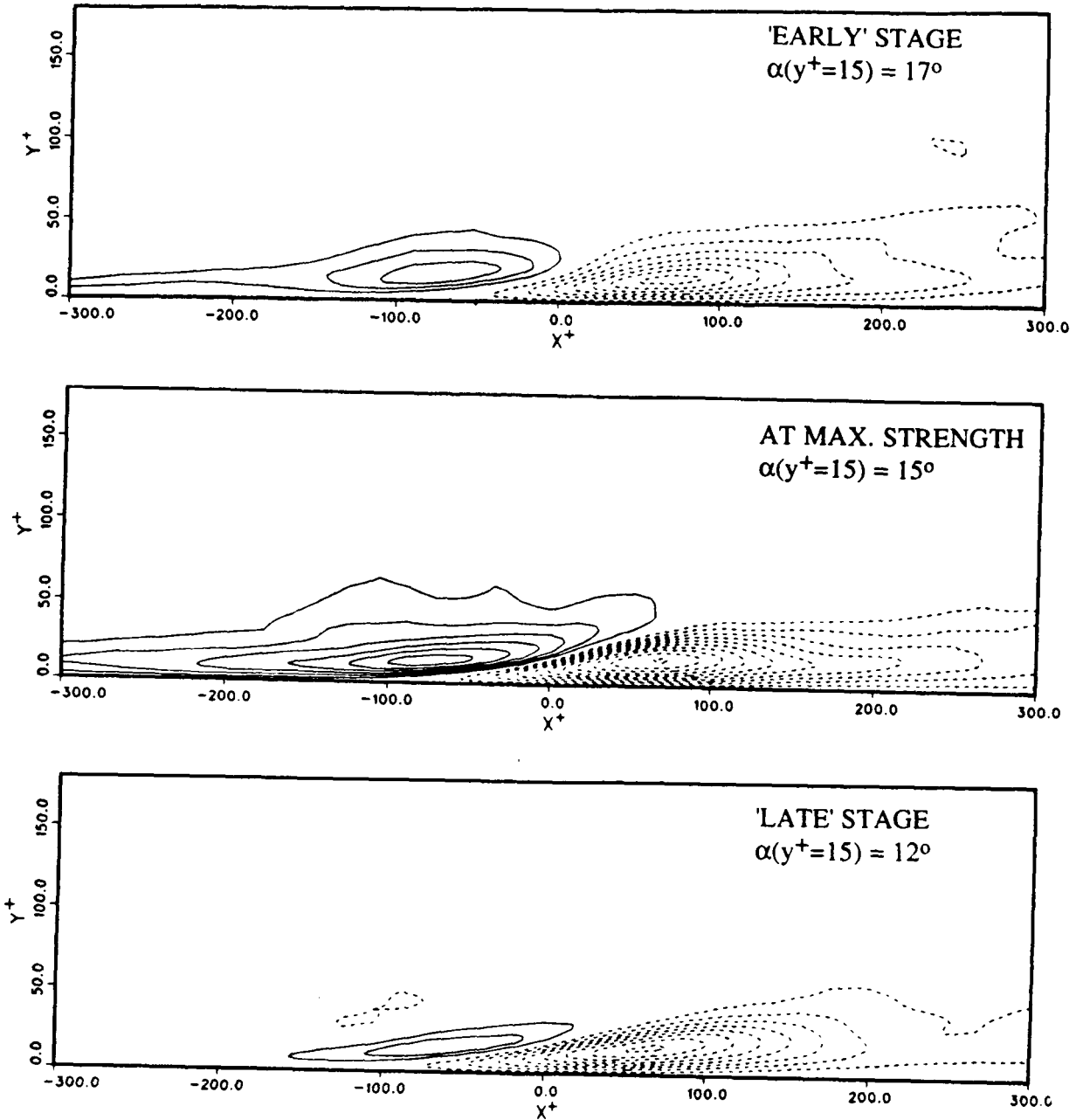
<u>

FIGURE 1.   VISA-educed conditional averages of the fluctuating part of the stream-
wise velocity in the xy-midplane of the structure at three stages of development.
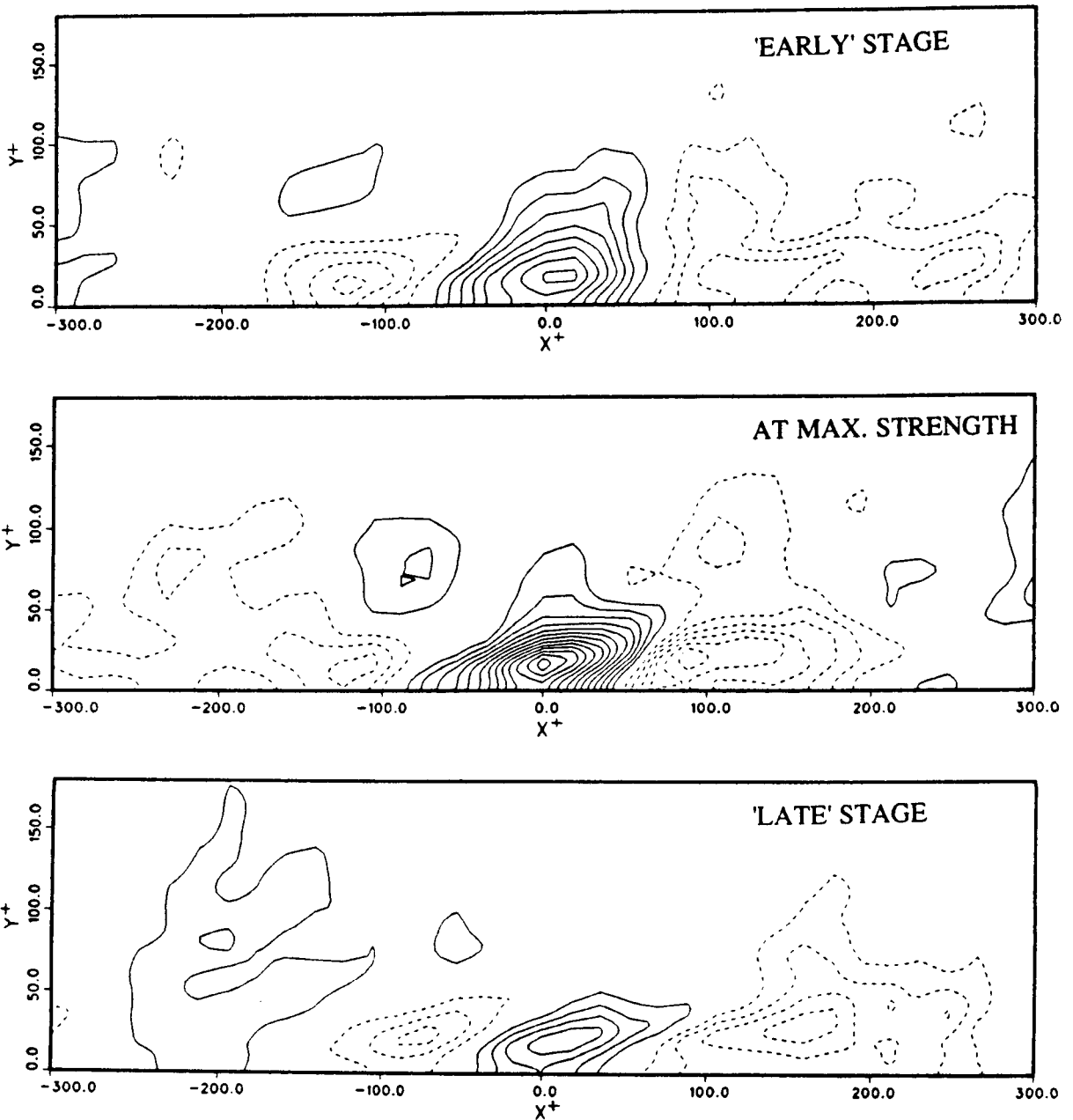Contour increment is $0.5u_\tau$, and dashed curves represent negative values.

$$<p-\bar{p}>$$

FIGURE 2. Conditional averages of the fluctuating part of the pressure ($< p - \bar{p} >$) in the xy-midplane of the structure at three stages of development. Contour increment is $0.2\tau_w$, and dashed curves represent negative values.
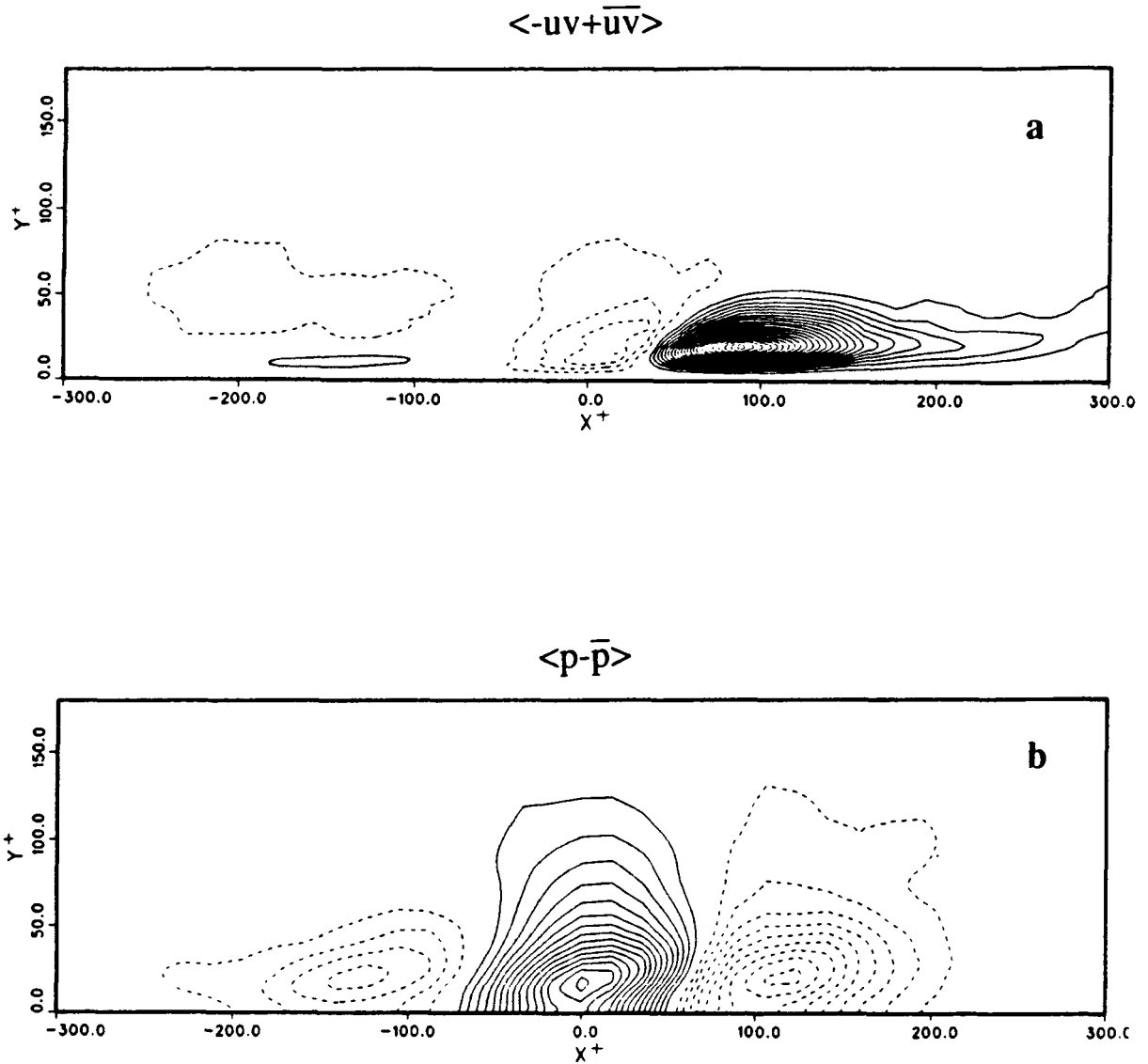
$$<-uv+\overline{uv}>$$

$$<p-\overline{p}>$$

FIGURE 3. Phase-aligned conditional averages of a) $< -uv+\overline{uv} >$ and b) $< p-\overline{p} >$ in the xy-midplane of the structure for all events detected at a chosen time. Contour increments are $0.2u_\tau^2$ and $0.2\tau_w$, respectively.

A cross-correlation technique was applied for 'phase-alignment' of the Reynolds shear stress and pressure patterns (figure 3). For the conditional average of all events detected at a chosen time, the maximum amplitude of the uv pattern (i.e. $< uv - \overline{uv} >$) increased by 35% to $4.2u_\tau^2$ as a result of the alignment. Similarly, the maximum pressure-amplitude increased by 37% to $2.7\tau_w$ after the alignment. Also the spatial coherence in the direction normal to the wall increased somewhat.
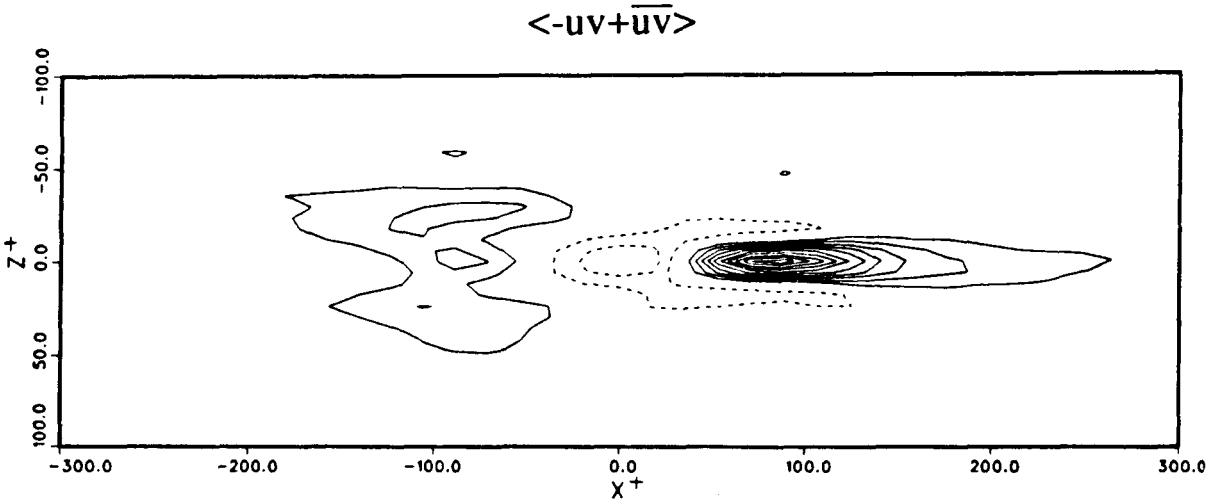
$$<\text{-uv+}\overline{uv}>$$

FIGURE 4. Conditional average of $< -uv + \overline{uv} >$ in the xz- plane of the structure at $y^+ = 15$ for all events detected at a chosen time. Contour increment is $0.2u_r^2$.

2.3 The role of spanwise asymmetry

Conventional conditional averaging schemes based on one-point detection yield averaged structures symmetric with respect to the xy- midplane when applied to flows with spanwise homogeneity. The conditional average of uv in a horizontal xz-plane at $y^+ = 15$, however, exhibits some interesting features, which indicate that the underlying individual realizations may perhaps not be symmetric (figure 4). The pattern has one lobe on each side of the $z = 0$ plane on the upstream side of the detection point, indicating that the the individual structures are predominantly asymmetric with respect to this plane. To test this hypothesis individual structures were followed in time. It was found that the strong shear often developed in a process where neighbouring elongated high- and low-speed regions interact through a localized spanwise motion, thus generating a flow structure with strong spanwise asymmetry.

In order to preserve this asymmetry in the construction of conditional averages a special scheme was devised, in which the individual structures were switched with respect to the xy-mid-plane (and reversing the sign of w) according to the sign of the spanwise derivative of u at the detection point. The resulting u-patterns in the $y^+ = 15$ plane, for the three stages of development described above, are shown in figure 5. The asymmetry is strongest at the stage of maximum strength of the shear-layer. This is indicative of the importance of spanwise asymmetry in the turbulence production processes, and it suggests that the evolution of near-wall flow structures is quite different from the generally accepted picture as of today.

A measure of the spanwise asymmetry can be obtained by examining the probability density distribution of $\partial u/\partial z$ at the detection point, i.e. at the position where $\partial u/\partial z$ is close to its maximum. In figure 6, the probability distribution of
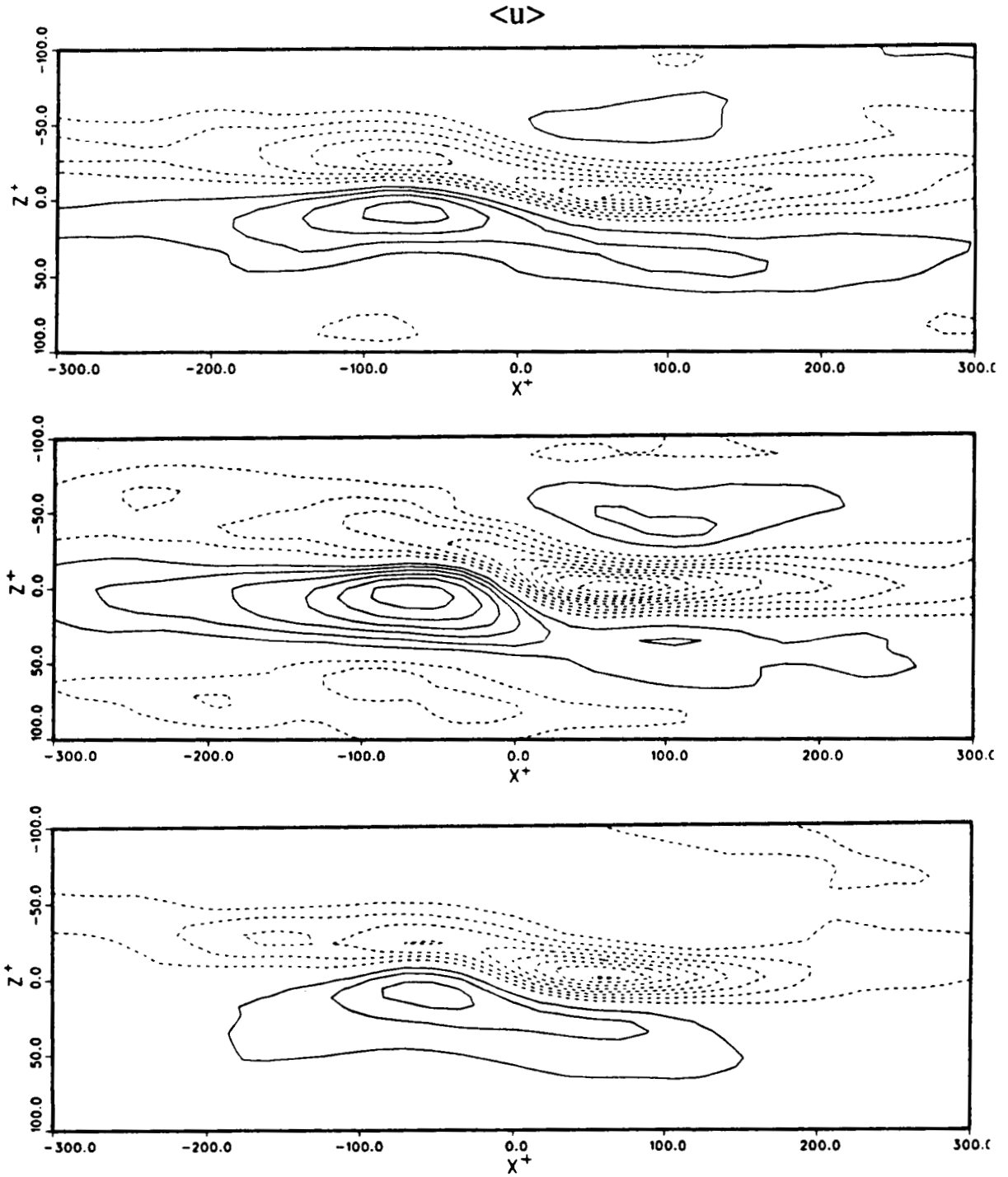
$\langle u \rangle$

FIGURE 5.   Conditional averages obtained with the modified VISA-method pre-
serving spanwise asymmetry. Patterns for the fluctuating part of the streamwise
velocity in the xz-plane of the structure at $y^+ = 15$ are shown at three stages of
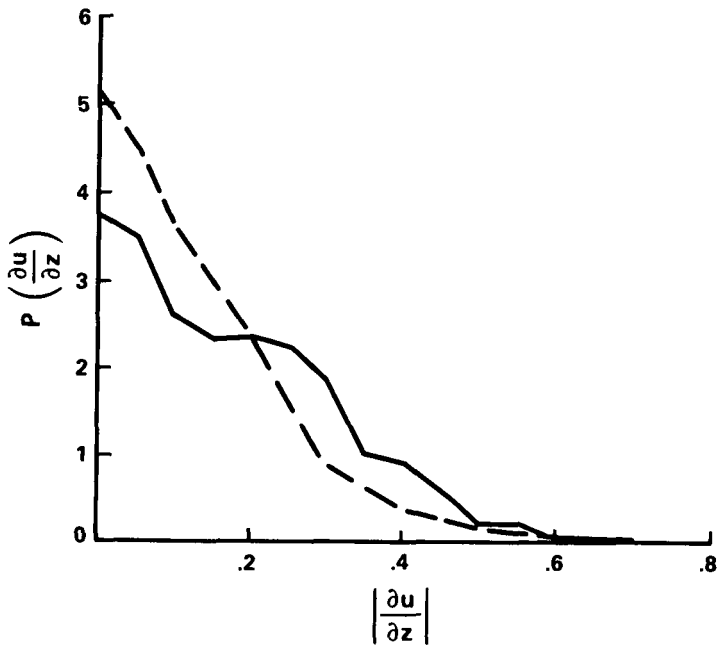development. Contour increment is $0.5u_\tau$.

FIGURE 6. Probability density distribution of $|\partial u/\partial z|$: ----, normal probability density with mean value of 0.11; ——, conditional probability density at VISA detection point with mean value of 0.20.

$\partial u/\partial z$ at the detection point obtained from twelve different velocity fields (about 700 events were detected in these fields) is compared with the overall probability density for the $y^+ = 15$ plane. The distribution of $|\partial u/\partial z|$ at the detection point is significantly wider than the normal one, illustrating the fact that large $\partial u/\partial z$ often are associated with the shear layers. The average value of $|\partial u/\partial z|$ at the detection point is about twice the overall-average value at $y^+ = 15$. The average value of $|\partial u/\partial z|$ at the detection point was found to be as large as 60% of the mean velocity gradient at $y^+ = 15$.

From the evolution of the asymmetric structures (figure 5), we note that the streaky pattern remains more or less intact throughout the process, indicating that there may not be a need for a further regeneration process for the low- and high-speed streaks.

2.4 Tracking of large-amplitude uv-peaks

The above results suggest a picture of the near-wall turbulence production process in which an important role is played by large- amplitude Reynolds stress peaks that are quite persistent in time in the Lagrangian frame of reference. Large uv-peaks were therefore tracked in space and time in a similar manner to that described for the tracking of shear-layers. We followed second quadrant uv-peaks with an amplitude larger than $4u_{rms}v_{rms}$ at a chosen time both forward and backward in time from that instant. The mean 'survival time' over which the amplitude exceeds
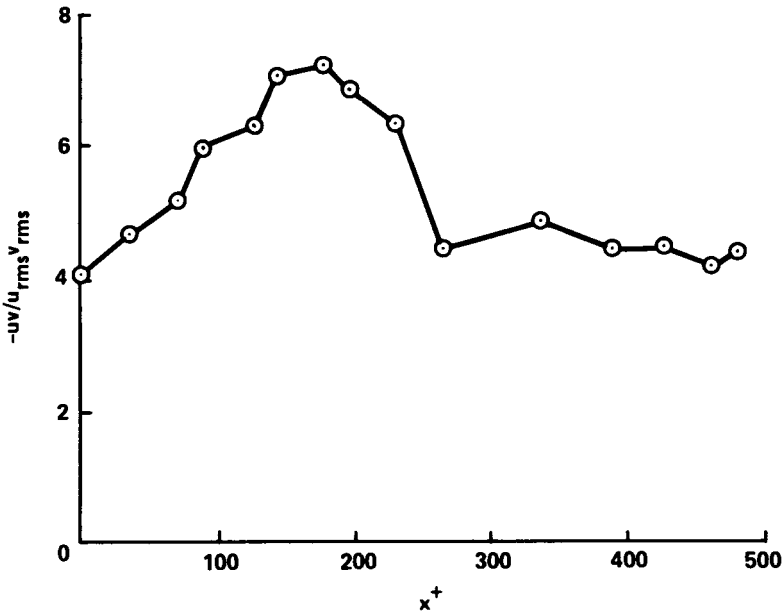
FIGURE 7. The amplitude of a second-quadrant uv-peak as it is followed over the period (45 viscous time units in this case) during which it has an amplitude larger than 4.0 $u_{rms}v_{rms}$.

the $4u_{rms}v_{rms}$ level was found to be more than 30 viscous time units. During this time the flow structure associated with this uv-peak has travelled more than 300 viscous length units (or 1.7 half channel heights). The example shown in figure 7 illustrates a uv-peak with an nondimensional amplitude above 4 over an interval of 45 viscous time units, during which it travelled nearly 500 viscous length units. In the Lagrangian reference frame the appearance of uv-peaks is spatially 'spotty', but certainly not intermittent in time. The average propagation velocity of the uv-peaks was found to be $9.9u_\tau$, comparable to that of the shear layer ($10.6u_\tau$).

3. Concluding remarks

The use of the NASA Ames numerical data bases has resulted in new insights into turbulence producing mechanisms in the near-wall region. The present study indicates that the commonly-held description of the turbulence production process needs some modification. The creation of small scales does not appear to be the major source of Reynolds stress or turbulent energy production; instead, a major source seems to be the persistent movement of low speed fluid out from the wall in front of the shear layer, which is a dominating feature of the flow in the near-wall region. The development of asymmetry in the spanwise direction seems to be an important component in shear-layer evolution, and suggests that an instability may take place between the high and low speed regions.

REFERENCES

BLACKWELDER, R.F. 1977 On the role of phase information in conditional sampling. *Phys. Fluids.* **20**, S232.

JOHANSSON, A.V., ALFREDSSON, P.H. & ECKELMANN, H. 1987a On the evolution of shear-layer structures in near-wall turbulence. In *Advances in Turbulence*, pp. 383-389, Proc. First European Turbulence Conference, Lyon, July 1986.

JOHANSSON, A.V., HER, A.V. & HARITONIDIS, J.H. 1987b On the generation of high amplitude pressure peaks in turbulent boundary layers and spots. *J. Fluid Mech.* **175**, 119.

JOHANSSON, A.V., ALFREDSSON, P.H. & KIM, J. 1988 Velocity and pressure fields associated with near-wall turbulence structures. In Proc. of the Zoran Zaric Memorial International Seminar on Near-Wall Turbulence, May 1988 Dubrovnik, Springer.

KIM, H.T., KLINE, S.J. & REYNOLDS, W.C. 1971 The production of turbulence near a smooth wall in a turbulent boundary layer. *J. Fluid Mech.* **50**, 133.

KLINE, S.J., REYNOLDS, W.C., SCHRAUB, F.A. & RUNSTADLER, P.W. 1967 The structure of turbulent boundary layers. *J. Fluid Mech.* **30**, 74.